Goddard Fabry-Perot and IFS

Users Manual

Version 1.0b (September 15, 2012)

Bruce E. Woodgate (NASA's GSFC), Carol A. Grady (Eureka Scientific & GSFC) George M. Hilton (USRA & GSFC), Timothy J. Norton (UMBC & GSFC) Michael W. McElwain (NASA's GSFC), Don Lindler (Sigma Space Corp. & GSFC), Ed Leon (NMSU), Ed Grabenhorst (Embry-Riddle Aeronautical University), Bryce Carpenter (Catholic University of America)

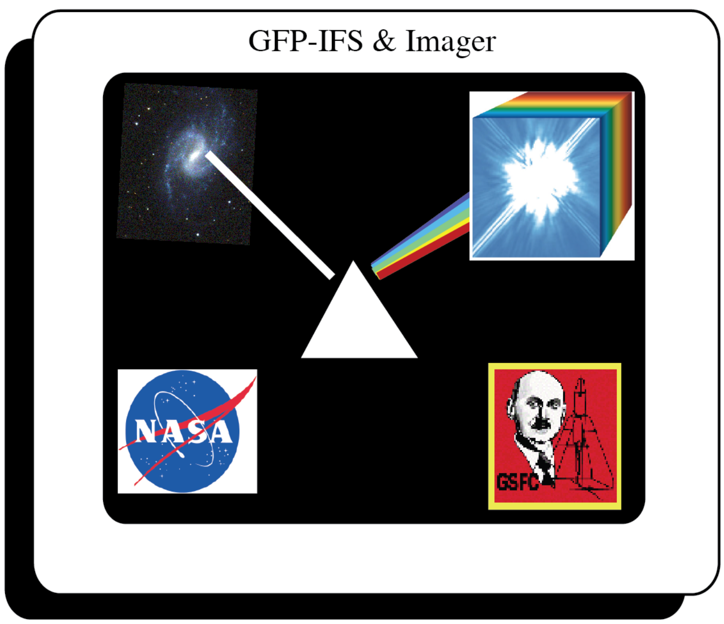

Table of Contents……………………………………………………………,,…………2

Appendices:

1. Introduction

The Goddard Fabry-Perot, IFS and Imager, is a visible-wavelength multi-purpose imager and imaging spectrograph for use in natural seeing at the Apache Point Observatory 3.5m telescope. As of September 2012, the instrument is available in direct imaging, coronagraphic imaging (using a wedge), and integral field spectroscopy modes.

The instrument is used at the Nasmyth 2 f/10.3 focus of the APO 3.5 m telescope. Behind the telescope focus, a field lens and collimator lens collimate the light through a clear optical path, or through specialty optics for an integral field spectrograph or a fabry-perot etalon. The instrument focus is wavelength-dependent, with different collimator settings needed to ensure sharp images. A filter or other element restricting the wavelength range imaged should always be in the optical path. Finally a camera lens refocuses the light onto the CCD, which currently can be used in a conventional analog mode.

Fig. 1-1: GIII mounted at Nasmyth 2 on the APO 3.5m telescope, with the instrument PI, Bruce Woodgate (photo courtesy M. McElwain).

1.1. Optical and Mechanical Design

The GIII is equipped with a suite of broad-band (FWHM~2000 Å) and medium band (FWHM~135 Å) filters for the 4000-10,000 Å range. As an imager, the system throughput including the CCD is TBD% in the red and TBD% in the blue.

Table 1-1: GIII Imaging Modes

Mode	Spatial Sampling	Fabry-Perot etalon	Wavelength Coverage	Spectral Resolution
Filter imaging	0.165”/pixel		4000- 10,000 Å	Set by filter
Coronagraphic filter imaging	“		4000- 10,000 Å	Set by filter

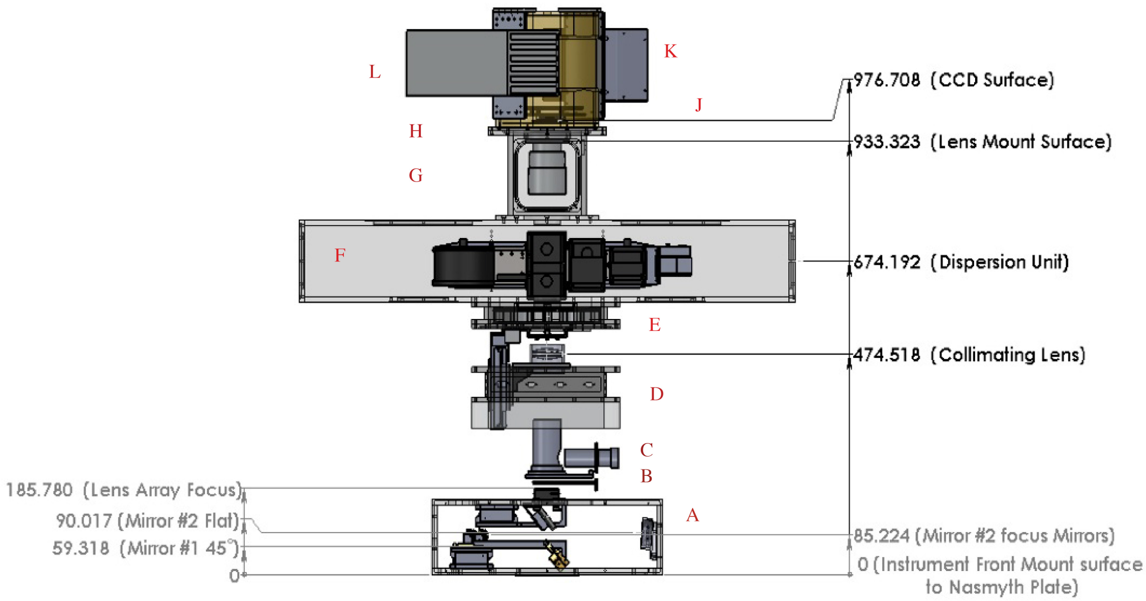

Fig. 1-2: SolidWorks view of GIII from bottom (telescope) to detector (top): Box A – (magnifier drive) houses IFS lenslets and associated optics, a coronagraphic wedge for direct imaging and a clear path for conventional filter and Fabry-Perot imaging. B is the manual slider for alternate coronagraphic spots. C is the location of the internal calibration system consisting of the integrating sphere, internal lamps and associated pickoff mirror. Box D houses the collimating lens and its associated focus drive. E is the filter wheel. F is the disperser drive housing IFS grisms, and a clear path for conventional imaging. G is the camera lens. H is the shutter assembly and camera lens mount. J is the CCD in its dewar. K is the Photon ETC controller for the CCD, while L is the Leach controller. The instrument focal plane is at the lens array focus just beyond box A for all modes, while the filter wheel is located near the pupil plane.

The instrument is used at the Nasmyth f/10.3 focus of the APO 3.5 m telescope. Supported modes include filter imaging and the IFS. Imaging modes are listed in table 1-1. IFS capabilities are listed in Table 1-2. The instrument is shown in Fig.1-1, with a SolidWorks diagram in Fig. 1-2.

GIII can also be configured as an IFS with fields of view intermediate in size between the imaging modes and the long-slit spectroscopy mode of DIS. The IFS operates in the green and red (λ≤7000 Å). Currently supported grisms are low resolution (R~1400-1800).

Table 1-2: . IFS Capabilities at the Apache Point Observatory 3.5-m Telescope

FOV (“x”)	Spatial Sampling (“)	Spectral Bandwidth (nm)	Spectral Sampling (nm)	λ_{cent} (nm)	Spectral Coverage	Mode*	Comments/ Lines in Range
Red:							600 l/mm grism
7x7	0.21	42	0.144	664	643-685	NSR	Hα [N II] [S II]
14x14	0.42	42	0.144	664	645-685	WSR	Hα [N II] [S II]
7x1.68	0.21	125	0.144	664	575-700	NLR	+[0 I] [S III] FeX He I
14x3.36	0.42	125	0.144	664	575-700	WLR	“
Blue/ Green:							810 l/mm grism
7x7	0.21	31	0.105	489	474-504	NSG	Hβ [O III]
14x14	0.42	31	0.105	489	478-504	WSG	“
7x1.68	0.21	107	0.105	489	433-540	NLG	+[O III] Fe XIV, Ar IV, He I, Cl III Fe III, He II Ne IV
14x3.36	0.42	107	0.105	489	433-540	WLG	“
10x2.4?	0.21?	45?	0.045?	660	630-675	Hires	[O I], FeX, Hα [N II] [S II]

*Mode descriptors: N or W for narrow or wide field; S or L for short or long spectrum; R or G for red or green band.
** Spectral regions around the short spectra ranges shown can be observed with nearby existing blocking filters (see Table 3-2).

1.2 Comparison with Other APO Facility Instruments

As an imager, GIII has a circular field of view which is only ~60% that of SPICAM. The main strength of GIII as an imager is the large suite of medium-band filters (FWHM=135Å), the availability of the coronagraphic wedge, and the Fabry-Perot mode. As an IFS, GIII offers contiguous 2-D spatial coverage of a field which is larger than the DIS slit widths, with higher spectral resolution than DIS, but with wavelength coverage limited to the green and red. DIS offers more complete (or user-specified) wavelength coverage, and simpler target acquisition and data analysis, at the expense of less complete spatial sampling near an object of interest.

Table 1-3 – Comparison with Other APO Facility Instruments

Instrument	Field of View	Filter Complement	Spectral Resolution
SPICAM	4.7′	SDSS u'g'r'i'z' MSSSO UBVRI	Few; set by bandpass
GIII- Imaging	2.8′ x2.8′ with some vignetting	BVRI, medium band, FP	Few (~2-3 for broadband), ~20 (grism blockers) 48 (medium band, red), 70 (Rutgers' Broad blockers), and higher for a few filters
DIS	1.5″, 2″, or 5″x 6′	Long-slit	300-400, 1200. 0.4-1.0 microns simultaneously
GIII-IFS	14″x14 ″or 7″x7″	IFS	R=1475 (green), 1823 (red), TBD (hi-res)

1.3 Instrument Operation

As of September 2012 GFP-IFS is operated through the log window in TUI using a suite of python scripts. All instrument configuration information is written into the fits headers, but telescope and environmental information is not yet available in the header. Telescope pointing, use of truss lamps, etc. are all managed through TUI. For TUI documentation see http://www.apo.nmsu.edu/35m_operations/TUI/). We anticipate that GFP-IFS will eventually be fully integrated into TUI.

Users of GFP-IFS should expect to have the observatory load filters prior to the observing time, configure the data directory on newton where data will be stored, and set permissions for TUI as for other instruments. Interim instructions for use of the python scripts are found in the document GFP_IFS _TUI _commanding.docx.

1.4. The NA2 Guide Camera

GFP-IFS has no dedicated guide camera, but uses the NA2 guide camera for guiding. See the SPICAM manual for details.

1.5 Focusing

If you are observing within the wavelength ranges of the IFS, the instrumental focus for GFP-IFS will be handled as part of the configuration of the instrument. Observers planning to use very red filters, which have yet to have measured instrumental focus (collimator) settings should contact the observatory well in advance of their observing time so that such data can be obtained for them.

Normally, the only focus settings that observers should be concerned about will be the telescope focus. GFP-IFS is focused in filter imaging mode by taking a suite of direct images with different 3.5m secondary positions. Changing these settings and determining the optimum focus is most efficiently executed with observing specialist assistance. Given the coarse sampling of the lenslet arrays and limited fields of view in the IFS modes we DO NOT recommend using IFS acquisition or spectral data for focusing the telescope. The focus procedure is the same as for SPICAM.

1.6 Image Orientation

Default GFP-IFS image orientation is North up (+y) and west to the right (+x) in filter imaging mode. The IFS field is rotated by 187.1° relative to the imaging field orientation. Alternate image rotations from the default N up, E to left can be specified using TUI. AS OF 9/12 ROTATION DATA ARE NOT RECORDED IN THE FITS HEADER AND WILL NEED TO BE DOCUMENTED BY OBSERVERS IN THEIR OBSERVING LOGS.

2. The Detector

GIII uses an e2v LLLCCD model 201 detector with 1024x1024, 13.3x13.3 micron^2 physical pixels. The CCD can be operated in conventional analog mode using a Leach GIII controller, The dewar is cooled with liquid N_2, and heated to a stable operating temperature using the Lakeshore 325 heater. Nominal operating temperature is 170K.

For more detail on EMCCDs in astronomy see (Ives, D. 2010) at indico.cern.ch/getFile.py/access?contribId=102&sessionId=10&resId=1&materialId=slides&confId=19099, or Tulloch & Dhillon 2010, arXiv 1009.3403.

2.1 Leach Electronics (Analog Mode) Operation (Default for GFP-IFS as of 9/12)

Clock and voltage parameters for the EMCCD are set via a timing-load file (.lod), which users will not normally access. The name of this file is recorded in the FITS header, in the event of problems requiring APO or Goddard team member troubleshooting. To identify which file was used to specify CCD parameters, the keyword

```
TIM_FILE= 'fw5_0.lod'          / timing-load file for CCD exposure
```

is in the exposure information section of the FITS header.

2.1.1 Detector Properties

Raw analog mode images have 1072 x1032 pixels. The dark strip on the left hand side of each image consists of 16 pixels of overscan plus 16 pixels of dark reference (i.e. aluminum covered pixels). On the right hand side of the image are another 16 pixels of overscan. The top of the image has another 8 row-wide dark reference strip. These strips can be used as alternates to dedicated bias frames or dark frames. The active image area corresponds to pixels x=33-1056, y=0 -1023 (Fig. 2-1).

2.1.2 Bias

With the current .lod file, the bias is near 2870 DN, and shows a 10 DN gradient from the top to the bottom of the image (Fig. 3), a 4 DN gradient along a row, as well as very low level horizontal banding (Fig. 3). With the Leach electronics, bias frames have a finite exposure duration of 100ms, and as a result individual bias frames have ~1-2 cosmic ray events. [average variance in a box 400:450x400:450 is 2.67 DN, average median in same box is 2870.54, average standard deviation is 1.44 DN].

Due to the gradients and presence of cosmic ray events, we suggest that users use a median of an odd number of bias frames to form a superbias rather than using the chip overscan region for bias estimation and removal.

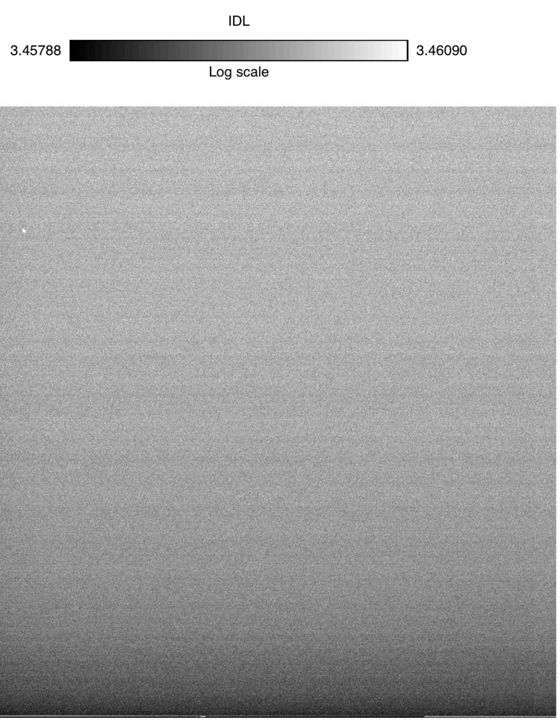

Figure 2-1: Scaled bias frame from December 2011. The bright spot in the upper left is a cosmic ray hit.

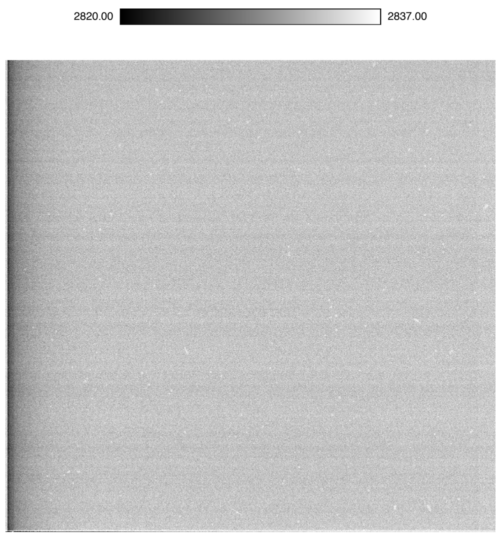

Figure 2-2 Median of 5 900s dark frames taken on 2012 01 10. With the exception of some residual signal from cosmic ray events, beyond the overscan region, the image is indistinguishable from bias frames.

2.1.3 Read Noise, Dark Current

Our model 201 EMCCD is a low read noise, and very low dark count detector when operated in analog mode using the Leach electronics. Nominal values for read noise are 2.88 e^- rms, with a gain of 2.3 e^-/ADU. The dark current is ~1e- /pixel/hour with no currently known dark patterns. To date, we have not found it necessary to obtain dark frames.

2.1.4 Linearity and Saturation

Full well for this detector is 80,000 e-. In ADU, the full well can be expressed as 34.78 Ke-/gain (figure 2-3). Bleeding in saturated images is along the +y detector axis.

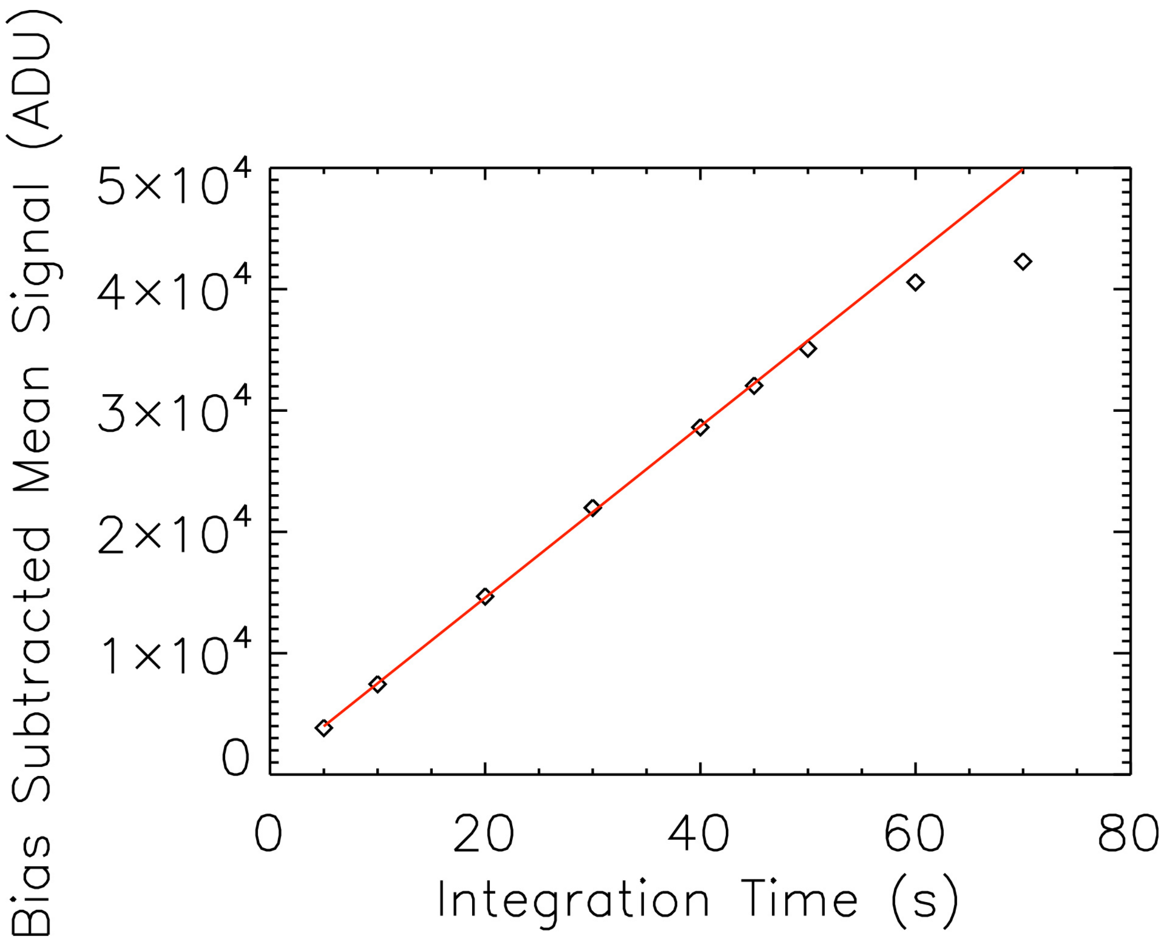

Figure 2-3: Detector response plotted against bright quartz truss lamp integration time, As measured for a 51x51 pixel box centered on (x,y)=(425,475). To ensure linearity, exposures should be kept under 34k counts. Standard deviations for each point plotted are smaller than the plot symbol used. To avoid saturation after lamp replacement in Feb. 2012, integration times should be 75% of the values shown above.

2.1.5 Readout

Using the Leach electronics, the GIII detector can be read out in 18s. Currently, only reading out of the full array is supported.

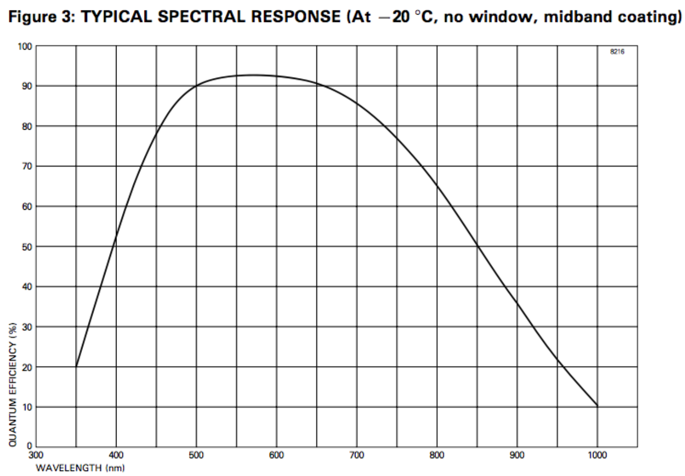

Figure 2-4: Typical e2v EMCCD 201 quantum efficiency (reproduced from the e2v specification).

2.1.6 Detector QE

The peak quantum efficiency of the CCD is 92% and typical spectral response is shown in Fig. 2-4. Additional performance details for the EMCCD 201 series are found in the detector manual (CCD201-20 Bl.pdf).

2.1.7 Vignetting and Detector Cosmetics

A flat field image taken with the 4861 Å IFS blocking filter and without (left) and with (right) the coronagraphic wedge in the optical path is shown in Fig. 2-6. The detector field shows some vignetting at the corners of the field of view. Light loss in the corners can reach 40% compared to the central portions of the detector. The detector used in GIII has no known hot pixels or bad columns as of January 2012. When the dewar was opened at APO in July 2011 however, some dust particles fell on the CCD, producing dark spots in any imagery where light falls on the detector. Table 2-1 lists the raw image (no overscan removal) coordinates of these features. The largest of these features is sufficiently small that conventional dithering should remove them for most direct imaging observations.

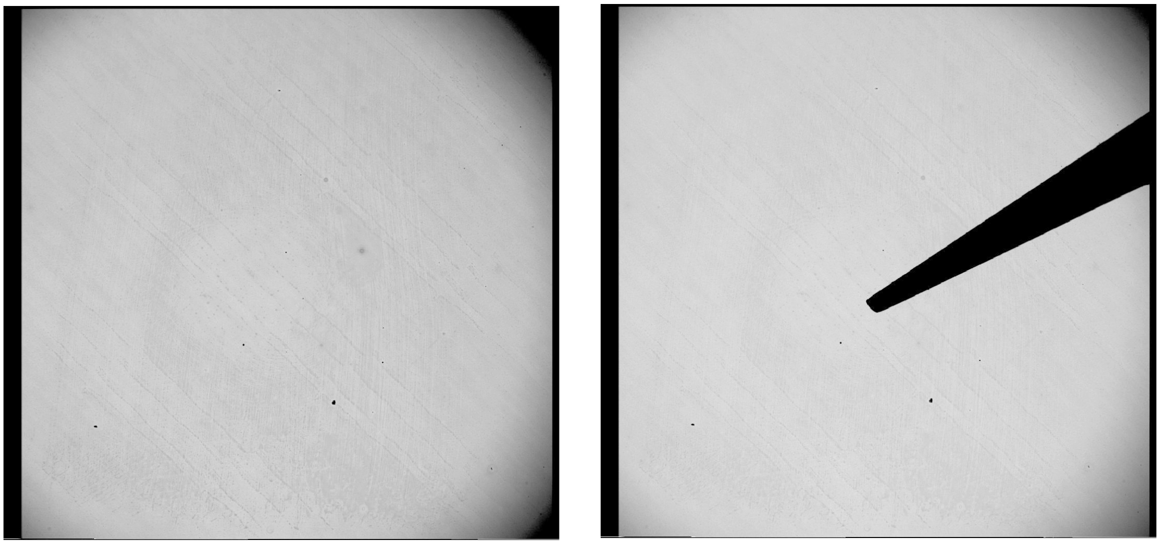

Figure 2-5 : Bright Quartz flat field images taken with the IFS blocking filter (λcen=4891Å), without (left) and with (right) the coronagraphic wedge in the optical path. Use of the wedge does not affect the amount of vignetting, which reaches ~40% at the extreme upper right of the image. The largest detector dust spots are also visible, with coordinates listed in Table 2-1. The 4891Å filter has some streaks at about 2-3% contrast: flat field data with S/N=100 should be routinely obtained if this filter is being used for imagery.

Table 2-1: Coordinates of Dust Specks in Raw Direct Images

X	Y
544	555
462	376
176	218
636	265
531	868
731	343
941	137

2.1.8 Fringing

Fringing is observed either in very narrow filters (FWHM=10 Å) or in very red filters.

2.1.9 Analog Mode Imaging Data Reduction

Imaging mode data reduction involves removal of the overscan and non-image strips, and bias subtraction. Cosmic ray events can be removed either by medianing an odd number (3 or more) similar exposures (e.g. IDL Median function), or using tools such as the IDL script la_cosmic.pro (see van Dokkum, P. 2001 PASP, 113, 1420 for the algorithm). Bright Quartz or sky flats can be used to compensate for pixel-to-pixel sensitivity variations. Data for photometric standard stars should be used to convert from ADU to flux. With the exception of the more complex non-image strip removal, the data reduction is similar to SPICAM.

3. GFP-IFS Filter Set

Due to its broad wavelength coverage and high quantum efficiency at long wavelengths, and wavelength-dependent focus, GFP-IFS must always be used with a blocking filter or dispersive element which restricts the imaging bandpass. GFP-IFS uses 50mm-diameter circular filters with thickness of 3-6 mm. The existing filter set includes broad-band (Table 3-1), as well as medium-band filters (FWHM 135-200 Å) and blocking filters for use with the IFS (4890/312 and 6645/419) in Table 3-2. Higher resolution blockers are listed in Table 3-3. The full filter set spans 4000-10,000 Å. Six filters can be mounted in GIII at one time. However, if users plan IFS operations, 3 of the 6 filter positions will be used for the IFS blocking filters, leaving only 3 free slots. As a result, we strongly suggest restricting observations to 1 IFS per half night (e.g. red or green, not both).

Filters noted as degraded have defects near the edge, which should be monitored for changes with time. Where known the manufacturer is specified to aid in locating filters in the storage boxes.

Table 3-1:GIII Broad Band Filters

Filter	Central wavelength	Manuf.	Quality
B	4400		
V	5300		
R	6000		
I	8000		Degraded 5mm in from edge

Table 3-2: Medium Band Filters

Name	Measured		Manuf.	Trans.	Qual.
	Central Wavelength	FWHM			
4015/50	4020	50	Andover	48%	
4050/160	4050	160			
4050/50	4050	57	Andover	47%	
4085/58	4086	58	Andover	48%	
4120/50	4124	52	Andover	49%	
4155/50	4156	50	Andover	46%	
4160/160	4160	160			
4200/135	4206	108	Andover	55%	
4257/100	4253	102	Barr	64%	
4300/135	4313	116	Andover	60%	Degraded 8 mm from edge

4400/135	4411	120	Andover	57%	Degraded 15mm from edge
4500/135	4507	122	Andover	66%	Degraded 15mm from edge
4600/135	4596	129	Andover	69%	Degraded 10mm from edge
4700/135	4701	109	Andover	76%	Degraded 10mm from edge
4760/100	4756	100	Barr	80%	
4800/135	4816	107	Andover	77%	Degraded 10mm from edge
4865/100	4864	91	Barr	81%	Degraded 8mm from Edge
4890/314	4890.7	313.9		99.06%	Green IFS blocker
4900/135	4909	105	Andover	72%	Degraded 4mm from edge
4982	4982	15			Degraded 5mm from edge
4994	4994	15			6mm, just one spot
5000/135	5007	106	Andover	74%	Degraded 4mm from edge
5007	5007	15-20			Degraded 6mm from edge
5007	5007	40			
5010	5011	106	Barr	74%	Degraded 3mm from edge
5020	5020	15			Degraded 5mm from edge
5032	5032	15			Degraded 8mm from edge
5100/135	5111	106	Andover	76%	Degraded 7mm from edge
5200/135	5210	116	Andover	72%	Degraded 10mm from edge
5265/115	5263	115	Barr	75%	Degraded 3mm from edge
5300/135	5304	86	Andover	71%	Degraded 5mm from edge
5340/135	5343	132	Barr	86%	Degraded 10mm from edge
5400/135	5406	124	Andover	74%	Degraded 5mm from edge
5500/135	5501	94	Andover	75%	Degraded 2mm from edge
5552	5549	138	Barr	77%	Degraded 8mm from edge
5600/135	5605	139	Andover	74%	Degraded 6mm from edge
5700/135	5703	139	Andover	74%	Degraded 2mm from edge
5800/135	5806	101	Andover	74%	Degraded 1mm from edge
5852/150	5845	154	Barr	88%	
5900/135	5902	109	Andover	76%	Degraded 1mm from edge
6000/135	6002	109	Andover	79%	Degraded 3mm from edge
6056/100			Andover		Degraded 5mm from edge
6052	6062	120	Barr	86%	
6100/135	6103	111	Andover	76%	
6235/135	6194	106	Andover	72%	???missing from Dave's list
6245/117	6235	117	Barr	94%	
6300/135	6307	126	Andover	69%	Degraded 3mm from edge
6400/135	6403	116	Andover	68%	Degraded 2mm from edge
6455/120	6450	119	Barr	96%	
6500/135	6512	122	Andover	74%	Degraded 10mm from edge
6563/117	6563	117	Barr	92%	
6645/418	6645.0	418		9896%	IFS red blocker
6564/10					
6600/135	6602	124	Andover	60%	Degraded 2mm from edge
6700/135	6698	124	Andover	60%	

6702/104	6702	124	Andover	63%	
6724/73	6724	73	Barr	?	
6766/138	6766	138	Barr	86%	
6800/135	6811	99	Andover	71%	Degraded 3mm from edge
6900/135	6891	102	Andover	62%	Degraded 3mm from edge
6945	6945	138	Barr	96%	
7000/135	7000	103	Andover	68%	
7100/200	7106	176	A-wd	95%	
7230/190	7230	190	Omega		
7240/185	7240	177	??	95%	
7360/185	7350	185	Andover	90%	
7480/185	7499	185	Andover	89%	Degraded 4mm from edge
7650/225	7650	212	Andover	92%	
7800/225	7785	218	Andover	98%	One side degraded
7950/225	7964	235	Andover	96%	
810.0	8101	223	Barr	96%	Degraded 5mm from edge
824.0	8228	206	Barr	96%	Degraded 6mm from edge
838.0	8368	244	Barr	92%	
852.0	8502	208	Barr	93%	
866.0	8668	218	Barr	94%	Degraded 8mm from edge
884.0	8829	262	Barr	92%	
902.0	9013	251	Barr	97%	Degraded 7mm from edge
920.0	9200	316	CS	85%	
938.0	9364	256	Barr	95%	
956.0	9580	266	Barr	95%	
977.0	9775	331	Barr	93%	
998.0	9978	329	Barr	90%	
1019.0	10220	348	Barr	94%	
10500	10500	200	SF		
10830	10830	200	A-wd		

Table 3-3: Blocking Filters for High Resolution

Name	Central wavelength	FWHM	Manufacturer	Throughput
4861/38	4861	38	Barr	
5007/40	5007	40	Barr	
6300/64	6300	64	Barr	
6563/69	6563	69	Barr	
6724/73	6724	73	Barr	

4. Field of View and Vignetting

The field of view and pixel scale on the sky are measured as part of the instrument block calibration establishing the location of the GFP-IFS relative to the NA2 guide camera frame. Nominal values are listed in the FITS header and in Table 4-1.

Table 4-1. Pixel and Spaxel Scales

Mode	Pixel or Spaxel Scale	Field of View
Conventional imaging	0.165″/pixel	169x169″ nominal
14″x14″ IFS	0.43″/lenslet	14.19x14.19″
7″x7″ IFS	0.215″/lenslet	7.09x7.09″

Regions affected by vignetting are shown in Fig. 2-5.

Table 4-2. Typical Direct Imaging Exposure Times:

Source type	Integration Time	Exposure level under photometric conditions
BD+28 4211, R=10.6, V=10.5 photometric standard star. Red grism blocker (6622, FWHM=419 Å)	5s	Peak single pixel 15k ADU over bias, Integrated over point source 1.12 E7 ADU
DG Tau, classical T Tauri star with strong emission lines, R=11.4, Hα medium band filter (FWHM=135 Å)	30s	Peak single pixel 22.2k ADU over bias, 9.38E5 ADU
Standard star, V=11.47 (HZ 44), green grism blocker	5s	Peak single pixel 6500 counts; integrated over source 366K

5. IFS

5.1 IFS summary

The GFP-IFS Integral Field Spectrograph (IFS) consists of two sections, the pre-formatter optics and the spectrograph. The pre-formatter section magnifies the image from the telescope focus onto a microlens array, so that the lenslets act as pixels sampling the image. This design follows the Tiger design concept (Bacon, R., et al. 1988, “The Integral Field Spectrograph TIGER”, in ESO conference “VLTs and their instrumentation”, Munich, March 1988), similar to OSIRIS at Keck (Larkin, J.E., et al. 2003, “OSIRIS: Infrared integral field spectrograph for the Keck adaptive optics system” SPIE, 4841, 1600.54), where spectra are interleaved between concentrated image points. The magnification can be altered to produce a field of view of 7 x 7″ or 14 x 14″. The magnifier is folded into the imaging portion of the GFP-IFS, and includes a field lens to feed a parallel beam into the microlens array There are 2 types of lenslet arrays in GFP-IFS. ***One microlens array has a pinhole array at its focal plane to reduce stray light and cross-talk between the spectra, awhile the other has no pinhole array and is suitable for faint objects.*** The pinhole array transmits only ~18.6% [40% - need to measure] of the light transmitted by the bare array, but can minimize saturation and straylight issues for brighter targets. The spectral format interleaves 8 spectra between each image point, with 4 pixels on the detector between each spectrum, resulting in spectra 196 pixels long for the full 33 x 33 spaxel image array onto a 1k x 1k detector. Longer spectra up to 828 pixels can be obtained using a slot mask for 33 x 8 lenslets behind the lenslet array, for a 7 x 1.2 or 14 x 2.4″ FOV (table 1).

The spectrograph optics use the existing Fabry-Perot optics (field lens, collimator lens, band-limiting filters in the existing filter wheel), a new camera lens to match image scales, and the photon-counting EMCCD. A grism mounted on the disperser drive behind the filter wheel in the parallel beam section allows change of spectroscopic bands and holds a Fabry-Perot etalon, as well as supporting a clear path for direct imaging. Each IFS disperser consists of a transmissive grating, between two prisms to return the dispersed light to its original path in both rotation and translation. The grisms use the VPH (Volume Phase Holographic) technology for highest throughput.

The lenslet arrays concentrate light into pupil images which can be observed directly, as in the target acquisition sequence for the IFS, or dispersed to produce a compact 2-D format. The lenslets are on a regular grid, and sample the image plane like a detector. In analogy with detector pixels, the lenslet images are termed “spaxels” in the rest of this document.

5.2. Acquiring Targets into the IFS field of view

The IFS field of view is much smaller than the direct imaging field of view, and requires a multi-step target acquisition process.

1. Image the field containing the target, preferably with the same filter that will be used in IFS observations. Locate the science target in the field of view, and measure its x, and y coordinates.

2. Offset the science target to the coordinates of the IFS aperture (Table 5-1) using TUI.

3. Take a confirming exposure to make sure the offset was in the correct direction.

4. Configure for IFS acquisition (lenslet array and blocking filter in optical path, grism out of optical path).

5. Take an exposure to locate your object in the IFS field of view, keeping in mind the 187° field rotation.

6. Adjust source placement in the field as needed, keeping in mind typical 3.5m

maneuver accuracies.

7. Put grism in the optical path.

8. Take spectral observation(s) with the science target interleaved with wavelength (truss lamp) observations.

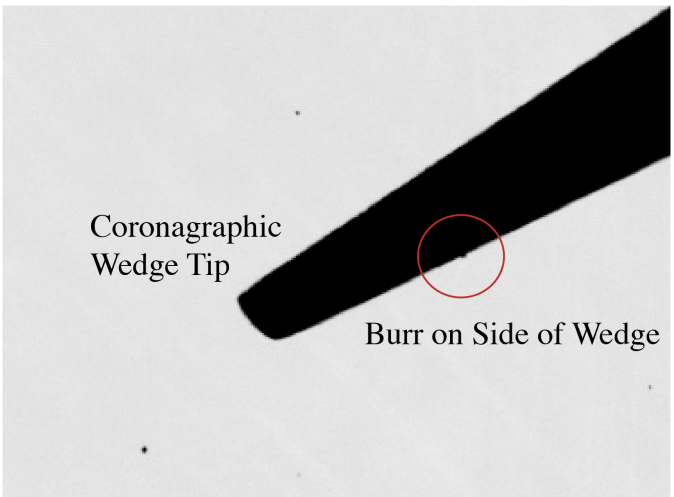

Figure 5-1: Location of the burr on the coronagraphic wedge which can be used to locate the center of the IFS field of view.

Table 5-1 Coordinates for Sweet Spot (IFS aperture) Location

Location	x	y
Sweet spot	550	434
Middle of coronagraphic wedge tip	519	444
Burr on side of wedge	632	479

The location of the IFS aperture is not immediately apparent in GFP-IFS direct images, but is just off the tip of the coronagraphic wedge. Pixel coordinates for this location are apt to change each time the instrument block is updated. As of late November 2011, the sweet spot/IFS aperture is located at (x,y)=(550,434). For the 14”x14” IFS field of view, a source placed at the tip of the coronagraphic wedge should be in the IFS field, after shifting to IFS mode. Alternatively, if the sweet spot needs to be located (e.g. after a new instrument block calibration), a small burr on the side of the wedge is a narrower fiducial point. From the burr, the center of the IFS field should be Δx, Δy= (-78, -45) pixels (see fig. 5-1 for the burr location).

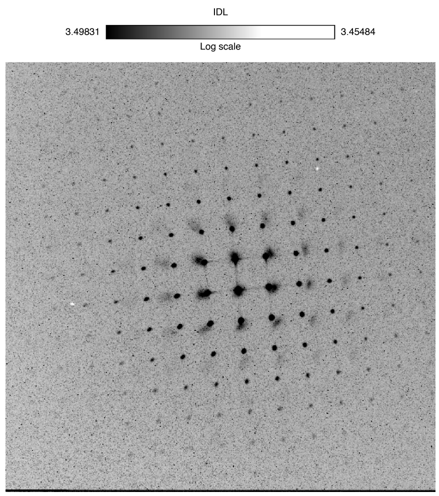

Figure 5-3: IFS acquisition imagery of a point source. (left) bare lenslet array for the T Tauri star DG Tau.with color table reversed. In addition to the individual lenslets, each lenslet is accompanied by diffraction spikes and ghost images (at the 1% level). These features are suppressed in pinhole array acquisition images. The region shown is 500 pixels on a side.

5.3 The IFS Optical Path

This section contains as-built optical diagrams for some of the IFS spectral modes, developed in Zemax.

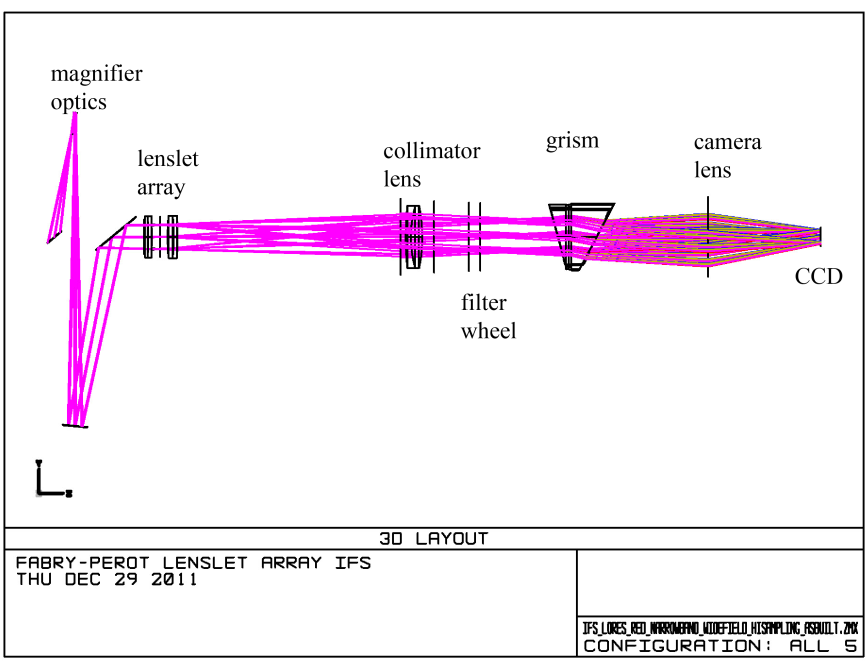

Figure 5-4: Simplified optical diagram for the red grism IFS mode.

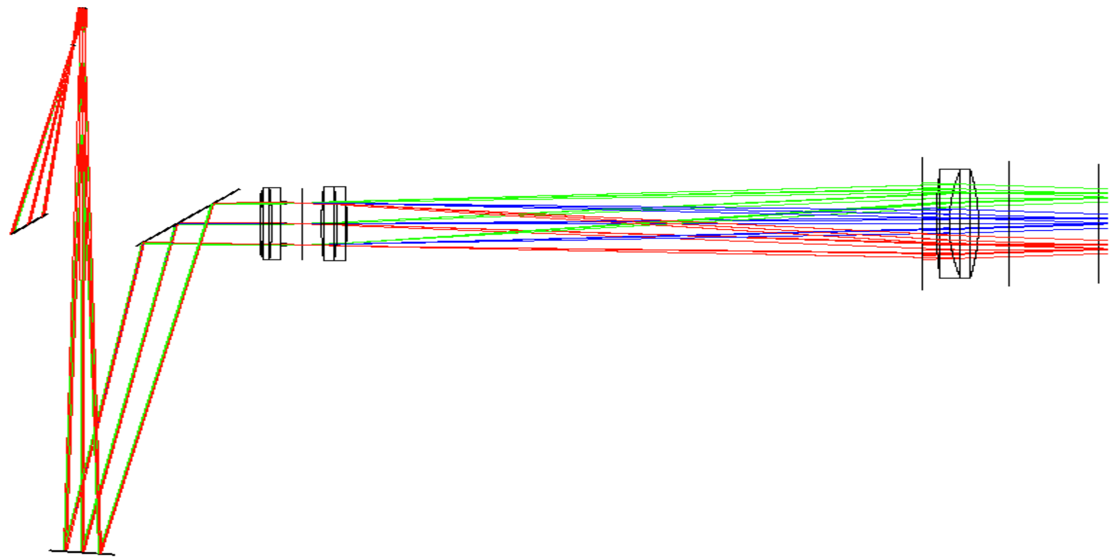

Magnifier optics Lenslet array collimator lens

Figure 5-5: expanded view of the front end of the IFS shown in Fig. 5-4.

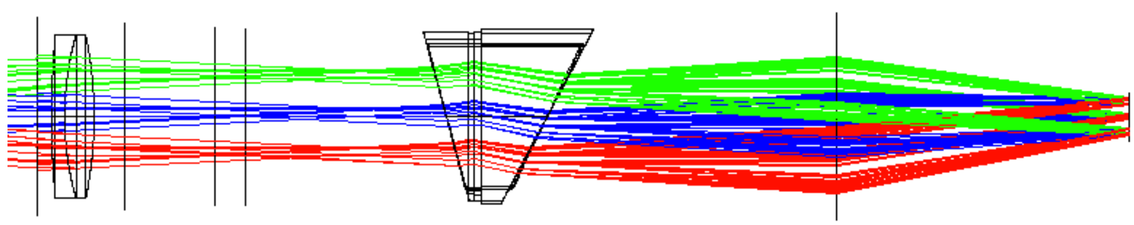

filter wheel grism camera lens detector

Figure 5-6: expanded view of the back end of the IFS shown in Fig. 5-4

5.4 Spectral Data

With the IFS grisms in the optical path, the instrument takes images with a dense 2-D format. A detail of a point source is shown in Fig. 5-7. Note the conspicuous H alpha emission in each spectral trace. A red grism composite image of a 30s Ne lamp exposure and a 30s Bright Quartz continuum (used to identify which emission lines go with what lenslet) is shown in Fig. 5-8.

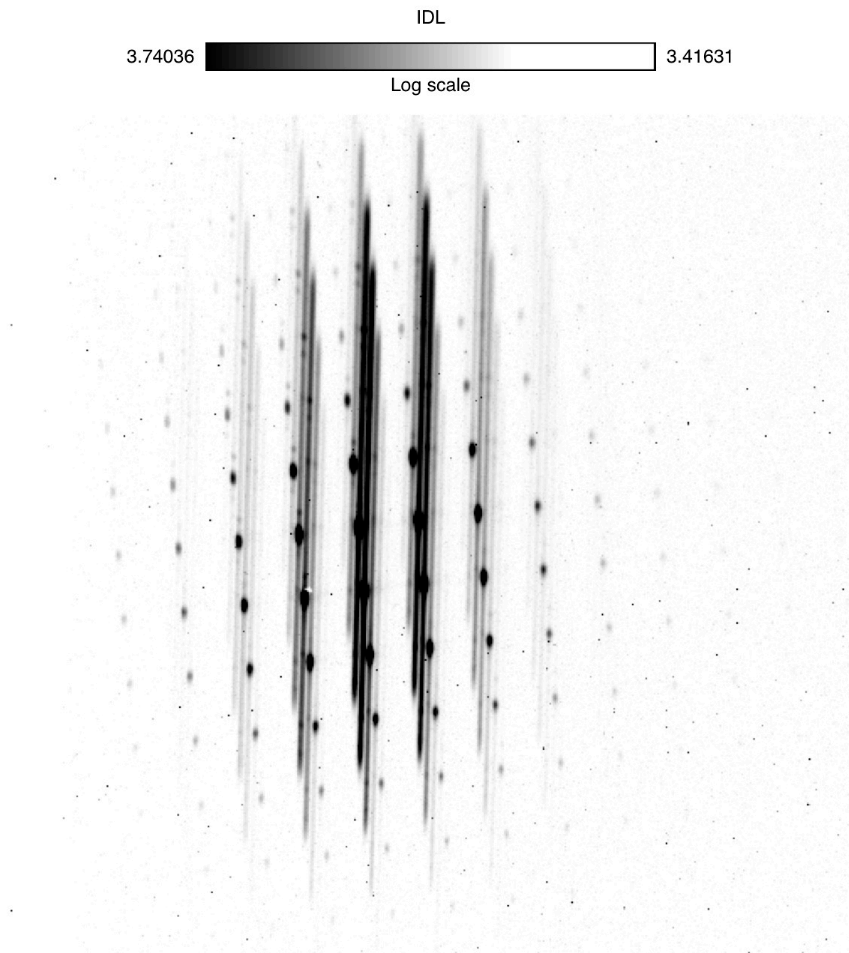

Fig. 5.7: Red grism spectrum of the classical T Tauri star DG Tau (reversed color table): Lenslet images are elongated in the y-direction, indicating that this R=11.4 object saturated slightly at H alpha. The spectrum associated with a single lenslet is aligned in the y-direction. [N II] emission lines flank H alpha. The more distant emission